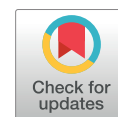**Biology Contribution**

# A Mouse Model for Microbeam Radiation Therapy of the Lung

Elisabeth Schültke, MD, PhD,[*] Sam Bayat, MD, PhD,[†,‡]
Stefan Bartzsch, PhD,[§,‖] Elke Bräuer-Krisch, PhD,[¶]
Valentin Djonov, MD, PhD,[#] Stefan Fiedler, PhD,[**]
Cristian Fernandez-Palomo, PhD,[#] Felix Jaekel, MD,[*]
Paolo Pellicioli, MSc,[¶] Verdiana Trappetti, MSc,[#]
and Guido Hildebrandt, MD, MSc[*]

*Department of Radiooncology, Rostock University Medical Center, Rostock, Germany; [†]STROBE
Laboratory, Grenoble Alps University, Inserm UA, Grenoble, France; [‡]Grenoble Alps University
Hospital, Grenoble, France; [§]Department of Radiooncology, Technical University Munich, Munich,
Germany; [‖]Institute for Innovative Radiotherapy, Helmholtz-Zentrum Munich (HMGU), Munich
Germany; [¶]European Synchrotron Radiation Facility, ID17 Biomedical beamline, Grenoble, France;
[#]Institute of Anatomy, University of Bern, Bern, Switzerland; and [**]European Molecular Laboratory
(EMBL), Hamburg, Germany

**Purpose:** Radiation therapy is an important treatment component for patients with lung cancer. However, the survival time gained with clinical radiation therapy techniques is relatively short. Data from preclinical experiments suggest that synchrotron microbeam radiation therapy could be much better suited to control malignant brain tumors than current clinical concepts of radiation therapy. Even at peak doses of several hundred gray, the extent of functional deficits is low.
**Methods and Materials:** We have developed the first mouse model to study the effects of microbeam irradiation in lung

tissue.

**Results:** Up to peak doses of 400 Gy, no acute adverse effects were seen.

**Conclusion:** This model is well suited to explore the potential of microbeam radiation therapy in the treatment of lung cancer and the response of normal lung tissue and organs at risk. © 2021 The Authors. Published by Elsevier Inc. This is an open access article under the CC BY-NC-ND license (http://creativecommons.org/licenses/by-nc-nd/4.0/).

## Introduction

Lung cancer is reported to have an incidence between 33.9 and 60 in 100,000, accounting for more than 10% of all new cancer cases annually.[1,2] For many of those patients, radiation therapy is an essential component of the interdisciplinary therapeutic approach.

Dose prescription to the lung is limited because of a high risk of pneumonitis, an inflammatory condition of the lung tissue caused by irradiation, which frequently results in lung fibrosis, leading to a severely reduced quality of life.[3] The fairly recent concept of stereotactic body radiation therapy offers patients with small lung tumors a much shorter treatment concept. However, such concepts are applicable only to a limited number of small peripheral lesions. High toxicity has been observed after treatment for central lesions.

Stereotactic radiation therapy works on the basis of spatial dose fractionation at the millimeter range. Throughout the past decades, the new concept of microbeam radiation therapy (MRT) has been developed in preclinical studies. MRT can be considered stereotactic radiosurgery with spatial dose fractionation at the micrometer range. In brain tissue, it has already been shown in small animal models of malignant brain tumors that the tumor control and normal tissue sparing achieved with MRT are superior to broad beam irradiation.[4-6] The better morphologic preservation of normal tissue structures resulted in well-sustained brain function in small and large animal models.[7,8]

Two phantom studies of microbeam irradiation in the lung were published in the 1990s.[9,10] We have designed and conducted the first feasibility study to investigate the acute response of lung tissue to microbeam irradiation in mice.

## Methods and Materials

The experiments were conducted at the biomedical beamline ID17 of the European Synchrotron Radiation Facility (ESRF) in Grenoble, France. All experimental protocols were approved by the Ethics Committee and by the French Ministry of Education and Research (permission number 7363-20l61 026150 13147).

A fixed space, multislit collimator, the design of which has been described in detail previously,[11] was inserted into the x-ray beam generated by the synchrotron source to generate an array of quasi-parallel microbeams. The result was an inhomogeneous dose distribution with periodically alternating sequences of peak dose (high dose) zones and valley dose (low dose) zones in the target tissue. The individual beam width was 50 µm and the center-to-center distance was 400 µm.

Before irradiating the animals, absolute dosimetry was performed following the protocol developed by Fournier et al.[12] The active volume of a PTW PinPoint ionization chamber (type 31014, PTW, Freiburg, Germany) was aligned in the center of a $20 \times 20$ mm$^2$ field and placed at 20 mm depth in a water-equivalent plastic cube phantom to determine the beam dose rate. The ionization chamber was calibrated with a TH200 radiation source to match the energy spectrum of the synchrotron radiation used in this experiment. The minimum field size measurable by the PinPoint chamber was respected. Under these reference conditions, the dose rate of the x-ray beam was determined in Gy/s/mA with an uncertainty of 4.4% ($2\sigma$). At the beginning of each irradiation procedure, the actual electron current of the synchrotron storage ring was considered to determine the dose rate in Gy/s to deliver the prescribed target dose.

Healthy male C57/BL6 mice obtained from Charles River France underwent microbeam irradiation of the right lung with an array of quasi-parallel microbeams. General anesthesia with isoflurane, tracheal intubation, and mechanical ventilation allowed reliable induction of an inspiratory apnea of a duration of approximately 10 seconds, sufficiently long to conduct microbeam irradiation at peak doses up to 400 Gy. The duration of the entire procedure, including the induction of anesthesia and intubation, positioning of the animal in the beam, and irradiation, ranged between 15 and 20 minutes.

Because no previous studies have examined the response of cardiac tissue and the impulse conduction system of the heart to high MRT peak doses, irradiation of the heart was avoided. Preirradiation imaging was conducted in irradiation position, and the position of the animal was corrected where necessary to ensure that the heart was outside the irradiation field (Fig. 1).

The typical alveolar structure of the lung with its multiple nonserial interfaces among air, fluid, and soft tissue makes dose calculation extremely challenging.[13] The peak and valley doses were calculated assuming a homogeneous mixture of water and air, where concentrations depended on the observed Hounsfield units of a computed tomography (CT) scan obtained with a spatial resolution of 197 µm using the CT component of a small animal positron
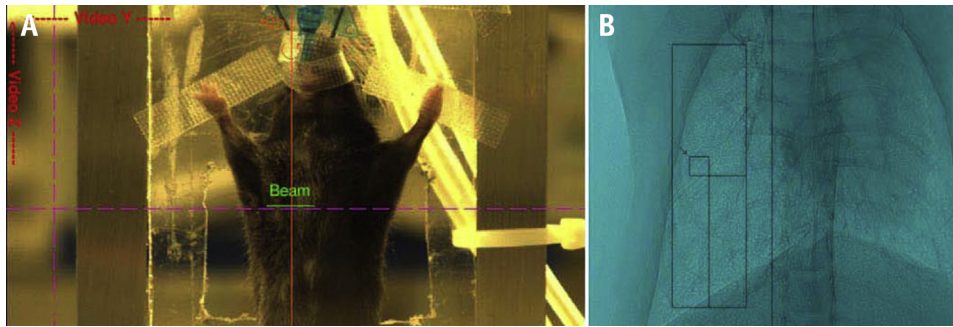
**Fig 1.**    Screen shot of the control room terminal with the animal positioned in the beam (A) and the preirradiation x-ray image (B), both with the beam array entry zone marked.

emission tomography/CT scanner (Inveon, Siemens). This CT scan was also used to outline the heart and the spinal cord as organs at risk. Monte Carlo calculation with the Geant4 tool package was conducted for a field size of 3.9 × 13 mm, corresponding to 9 vertical microbeams, in the right lung of the animals. Uncertainties of the Monte Carlo simulations for peak and valley doses are estimated below 7%. A more detailed description of the experimental setup is provided as supporting material.

## Results

We conducted a pilot experiment with 2 different peak doses (n = 18/group). The peak entrance doses were 40 Gy and 400 Gy and the valley doses were nominally 0.42 Gy and 4.2 Gy, respectively. Thus, the peak-to-valley dose ratio at the beam entrance was approximately 95 at a depth of 3 mm. The dose on the heart, the most important organ at risk with irradiation of the thoracic cavity, was calculated to be on average 0.11 Gy for a peak dose of 40 Gy and 1.1 Gy for a peak dose of 400 Gy (Fig. 2).

No signs of potential adverse effects owing to pulmonary or cardiac toxicity, such as audible breath sounds, pulmonary distress, or decrease in general activity, were seen in the mice at any time during the 72-hour observation period after microbeam irradiation. No motor deficits as signs of spinal cord toxicity were observed. The

observation was conducted continuously for approximately 1 hour after irradiation in a wake-up room setting, in 2-hour intervals for the following 8 hours, and 3 times daily thereafter.

Aiming for a constant post-end-expiratory pressure during irradiation, we were able to standardize the experiment throughout all experimental groups. Furthermore, we also successfully standardized the harvest of the lung tissue, to reproduce the irradiation morphology as close as possible. The gamma H2AX immunostain, representing the number of DNA double-strand breaks caused by the irradiation, resulted in intense fluorescence along the microbeam paths in all irradiated groups. After irradiation with peak doses of 400 Gy, the intensity of the immunofluorescence increased continuously during the first 3 days after irradiation (Fig. 3 and Fig. E3). This can be explained by delayed cell death due to secondary processes, including radiation-induced bystander effects. The intensity of the gamma H2AX stain along the microbeam paths is significantly lower after irradiation with peak doses of only 40 Gy.

## Discussion

This was the first time that the lung of mice was chosen as target organ for microbeam irradiation. We have shown that
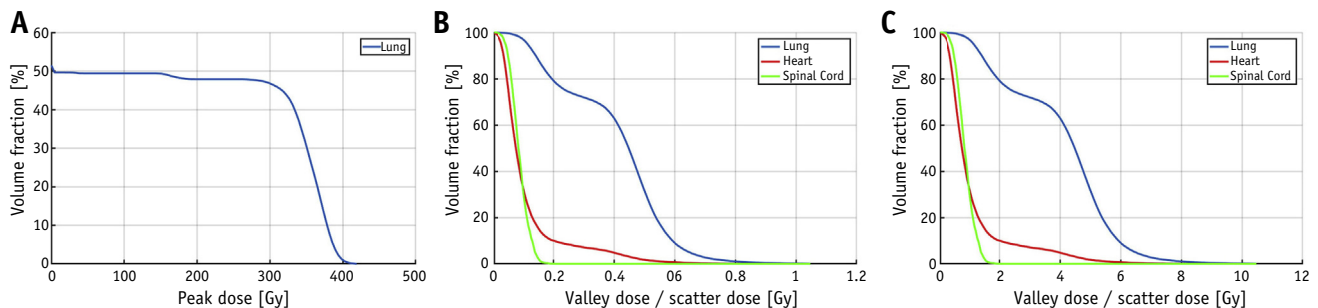


**Fig 2.**    Dose-volume histogram (DVH) for peak dose and valley doses expected for the nonirradiated lung, the heart, and the spinal cord after microbeam irradiation with peak doses of 40 Gy (B) and 400 Gy (C). Similar to the valley dose curves, the shape of the curves for peak doses of 40 Gy and 400 Gy is identical, but the values differ by a factor of 10.
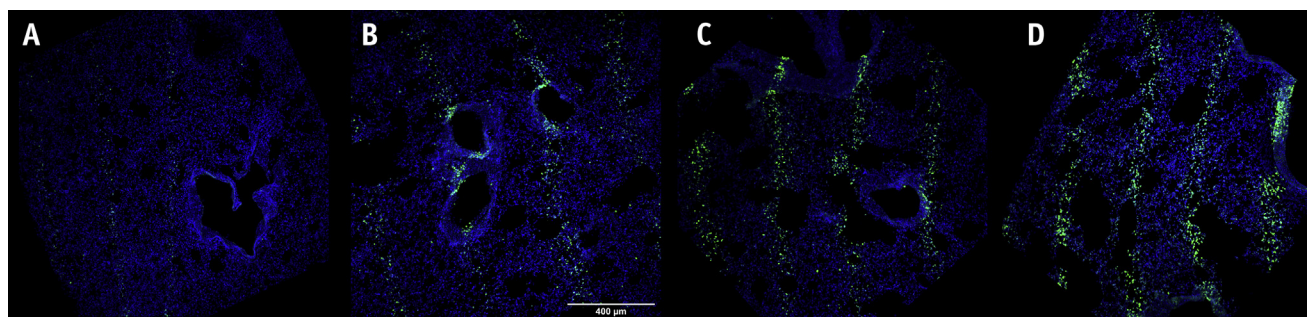
**Fig 3.**    Microphotographs of lung tissue after gamma H2AX immunostain. The staining intensity is much less intense at 24 hours after irradiation with peak doses of 40 Gy (A), compared with 400 Gy (B). The staining intensity increases continuously until the end of the observation period at 72 hours after irradiation, as shown in the immunofluorescence images at 48 hours (C) and 72 hours (D) after irradiation with peak doses of 400 Gy.

no acute adverse effects occurred after MRT with peak doses up to 400 Gy.

In the present study, the irradiation dose was based on Monte Carlo simulations designed to simulate both the reference conditions and the irradiation geometry in the animals. An experimental dosimetry study for the microbeam irradiation was not performed. The development of specific phantoms to reproduce the irradiation geometry in the animals in combination with high-resolution detectors could be an interesting theme for future studies.

The diameter of an alveolus, the structural unit in which gas exchange takes place, is about 200 μm in humans and 35 to 45 μm in mice.[14] Thus, dose calculation in human patients might be somewhat easier with respect to the changes of air/fluid/soft tissue interfaces, but more demanding because of the increase in scatter expected in the larger target areas in human patients, which would result in a decrease in the peak-to-valley dose ratio.[10]

To allow irradiation of irregularly (not rectangular) shaped targets without risking functional cardiac damage, the experimental setup should be refined. One could introduce a multileaf collimator, which allows temporary blocking of microbeam paths in analogy to clinical radiation therapy. Another solution might be the insertion of a radio-opaque mask protecting the heart.

Provided that a low toxicity profile can be shown in long-term studies after MRT in the lung, we suggest testing a scenario in which MRT is used as a simultaneously integrated boost in a clinical radiation therapy schedule to achieve a higher single-fraction dose. Clinically, the simultaneously integrated boost concept has been shown to result in longer local recurrence-free survival in patients with NSCLC.[15] This could be an especially interesting approach in patients with a low percentage of PD-L1−positive tumor cells reported in the initial histology.

A high percentage of PD-L-1−positive cells within a tumor correlates to a high responsiveness of the tumor to newly developed checkpoint inhibitors and thus to better tumor control and longer survival times.[16] Recent data suggest that hypofractionated radiation therapy might support the induction of PD-L1. This radiation

therapy−induced PD-L1 expression has been reported to be stable and long-lasting in vitro as well as clinically.[17-19] MRT can be considered a hypofractionated radiation therapy approach par excellence, with between 1 and 3 fractions reported in the literature. It would be interesting to follow up the work hypothesis that MRT induces the check point inhibitor PD-L1 and thus improves tumor responsiveness to immunotherapy.

With its extremely good preservation of normal tissue function observed previously in brain tissue, MRT might also prove to be a good approach to increase both the quality of life and the recurrence-free interval for patients with lung cancer.

## Conclusion

Microbeam irradiation studies in the lung of mice are technically feasible, albeit technically challenging. The mouse model can therefore be considered a suitable tool for further preclinical studies focused on the treatment of lung cancer and the study of normal tissue tolerance.

## References

1. World Cancer Research Fund International. Available at: www.wcrf.org. Accessed 07, 2020.
2. Death Cause Statistics 2013. Wiesbaden, Germany: Federal Agency for Statistics; 2014.
3. Schröder C, Engenhart-Cabillic R, Vorwerk H, et al. Patient's quality of life after high-dose radiation therapy for thoracic carcinomas: Changes over time and influence on clinical outcome. *Strahlenther Onkol* 2017;193:132-140.
4. Potez M, Bouchet A, Flaender M, et al. Synchrotron x-ray boost delivered by microbeam radiation therapy after conventional x-ray therapy fractionated in time improves F98 glioma control. *Int J Radiat Oncol Biol Phys* 2020;7:360-369.
5. Bouchet A, Potez M, Coquery N, et al. Permeability of brain tumor vessels induced by uniform or spatially microfractionated synchrotron radiation therapies. *Int J Radiat Oncol Biol Phys* 2017;98:1174-1182.
6. Bouchet A, Bräuer-Krisch E, Prezado Y, et al. Better efficacy of synchrotron spatially microfractionated radiation therapy than uniform radiation therapy on glioma. *Int J Radiat Oncol Biol Phys* 2016;95:1485-1494.

7. Schültke E, Juurlink BH, Ataelmannan K, et al. Memory and survival after microbeam radiation therapy. *Eur J Radiol* 2008;68(3 Suppl): S142-S146.

8. Laissue A, Blattmann H, Wagner HP, Grotzer MA, Slatkin DN. Prospects for microbeam radiation therapy of brain tumours in children to reduce neurological sequelae. *Dev Med Child Neurol* 2007;49: 577-581.

9. Company FZ, Allen BJ. Calculation of microplanar beam dose profiles in a tissue/lung/tissue phantom. *Phys Med Biol* 1998;43:2491-2501.

10. Company FZ. Calculation of dose profiles in stereotactic synchrotron microplanar beam radiotherapy in a tissue-lung phantom. *Australas Phys Eng Sci Med* 2007;30:3-41.

11. Bräuer-Krisch E, Requardt H, Brochard T, et al. New technology enables high precision multislit collimator for microbeam radiation therapy. *Rev Sci Instrum* 2009;80.

12. Fournier P, Crosbie JC, Cornelius I, et al. Absorbed dose-to-water protocol applied to synchrotron-generated x-rays at very high dose rates. *Phys Med Biol* 2016;161:N349-M361.

13. Hombrink G, Wilkens JJ, Combs SE, Bartzsch S. Simulation and measurement of microbeam dose distribution in lung tissue. *Physica Medica* 2020;75:77-82.

14. Soutiere SE, Tankersley CG, Mitzner W. Differences in alveolar size in inbred mouse strains. *Respir Physiol Neurobiol* 2004;140:283-291.

15. Qiu B, Li QW, Ai XL, et al. Investigating the loco-regional control of simultaneous integrated boost intensity-modulated radiotherapy with different radiation fraction sizes for locally advanced non-small-cell lung cancer: Clinical outcomes and the application of an extended LQ/TCP model. *Radiat Oncol* 2020;15:124.

16. Guirgis HM. The impact of PD-L1 on survival and value of the immune check point inhibitors in non-small-cell lung cancer: Proposal, policies and perspective. *J Immunother Cancer* 2018;6:5.

17. Narits J, Tamm H, Jaal J. PD-L1 Induction in tumor tissue after hypofractionated thoracic radiotherapy for non-small cell lung cancer. *Clin Transl Radiat Oncol* 2020;22:83-87.

18. Gong X, Li X, Jiang T, Xie H, Zhu Z, Zhou F, Zhou C. Combined radiotherapy and anti-PD-L1 antibody synergistically enhances anti-tumor effect in non-small cell lung cancer. *J Thorac Oncol* 2017;12: 1085-1097.

19. Shen MJ, Xu LJ, Yang L, Tsai Y, Keng PC, Chen Y, Lee SO, Chen Y. Radiation alters PD-L1/NKG2D ligand levels in lung cancer cells and leads to immune escape from NK cell cytotoxicity via IL-6-MEK/Erk signaling pathway. *Oncotarget* 2017;8:80506-80520.